Diurnal Ocean Surface Layer Model Validation

Jeffrey D. Hawkins
Douglas A. May
Remote Sensing Branch
Ocean Sensing and Prediction Division
Ocean Science Directorate

Fred Abell, Jr.
Sverdrup Technology, Inc.

Approved for public release; distribution is unlimited. Naval Oceanographic and Atmospheric Research Laboratory, Stennis Space Center, Mississippi 39529-5004.

Foreword

Numerous naval applications are directly dependent on knowing the past, present, and future sea surface temperature (SST) fields. The Diurnal Ocean Surface Layer (DOSL) model at the Fleet Numerical Oceanography Center attempts to fill a portion of these requirements by forecasting the 24-hour change in global SSTs. This procedure is done by using the wind stress and heat flux forcing functions available from the Naval Operational Global Atmospheric Prediction System as input to the parameterized DOSL model.

This report deals with validating the DOSL products using infrared imagery obtained in several locations during the night and day to map the diurnal SST changes. Particular attention is focused on extreme diurnal warming events, since these cases are most commonly associated with surface mixed-layer warming that disrupts the surface acoustic duct. Several events are detailed in the subtropical Atlantic to depict the capabilities within the DOSL model.

W. B. Moseley
Technical Director

J. B. Tupaz, Captain, USN
Commanding Officer

Executive Summary

The Diurnal Ocean Surface Layer (DOSL) model at the Fleet Numerical Oceanography Center forecasts the 24-hour change in global sea surface temperatures (SST). Validating the DOSL model is a difficult task due to the huge areas involved and the lack of in situ measurements. Therefore, this report details the use of satellite infrared multichannel SST imagery to provide day and night SSTs that can be directly compared to DOSL products. This water-vapor-corrected imagery has the advantages of high thermal sensitivity (0.12°C), large synoptic coverage (nearly 3000 km across), and high spatial resolution that enables diurnal heating events to be readily located and mapped.

Several case studies in the subtropical North Atlantic readily show that DOSL results during extreme heating periods agree very well with satellite-imagery-derived values in terms of the pattern of diurnal warming. The low wind and cloud-free conditions necessary for these events to occur lend themselves well to observation via infrared imagery. Thus, the normally cloud-limited aspects of satellite imagery do not come into play for these particular environmental conditions.

The fact that the DOSL model does well in extreme events is beneficial from the standpoint that these cases can be associated with the destruction of the surface acoustic duct. This so-called "afternoon effect" happens as the afternoon warming of the mixed layer disrupts the sound channel and the propagation of acoustic energy. Thus, the DOSL model can be used to help estimate the location of where the afternoon effect may occur, as well as help analysts interpret artificially induced, diurnal heating SST gradients when generating mesoscale front and eddy maps.

Acknowledgments

The author gladly acknowledges the many contributions that made this effort possible. M. Clancy, Fleet Numerical Oceanography Center, provided operational Navy diurnal sea surface temperature and marine wind field products. E. Arthur, Naval Ocean Research and Development Activity (NORDA), acquired NOAA-9 infrared imagery via NORDA's Satellite Digital Receiving and Processing System.

M. Clancy and J. Price (Woods Hole Oceanographic Institution) provided consultation on all aspects of the DOSL model and mixed-layer thermodynamics.

This work was supported by the Chief of Naval Operations (OP-096), the Space and Naval Warfare Systems Command, and the Satellite Applications and Techniques program, Program Element No. 63704N, LCDR W. A. Cook, Program Manager.

Contents

Diurnal Ocean Surface Layer Model Validation

I. Introduction

The U.S. Navy requires a wide range of real-time sea surface temperature (SST) analyses (nowcasts) and forecasts to meet the increasingly sophisticated needs demanded by sensors and weapon systems. The SSTs may directly or indirectly impact successful and efficient completion of duties ranging from antisubmarine warfare (ASW), optimum track ship routing, and search and rescue, or serve as vital input to atmospheric prediction models that require accurate air-sea interface initial conditions. This report focuses on the validation of one model aimed at satisfying the need to forecast daily SST changes.

The Diurnal Ocean Surface Layer (DOSL) model (Clancy, 1986) is run daily at the Fleet Numerical Oceanography Center (FNOC) in Monterey, CA, and predicts the daily SST changes due to the impact of surface heat fluxes and wind stress. This parameterized model requires no SST initial conditions and uses the forecast winds and fluxes from the Navy's global atmospheric model to provide the key input parameters. It then produces a prediction for the diurnal SST heating that is valid globally at the time of local maximum heating.

The DOSL model thus generates a contoured map for both hemispheres outlining the regions of large diurnal heating. This graphical guidance can be used to outline areas where the surface acoustic duct may be lost due to solar-heating-induced stratification (afternoon effect); to help correctly interpret infrared SST or forward-looking infrared images for ocean mesoscale feature locations; and to delineate regions where day and night satellite SSTs should not be mixed, since they represent two totally different environmental conditions. The DOSL model can thus provide some unique capabilities when properly used in conjunction with the right Navy mission.

Validating a prognostic SST model over large time and space scales (DOSL uses a polar stereo grid of ~ 320 km and is interpolated to a 2.5° × 2.5° grid) raises several interesting problems. It is not sufficient to match individual point values with in situ measurements, since the pattern of SST warming is also a key output value. Therefore, accurate SST reports within regional and sometimes basin scale domains must be combined with the attribute of coincident timing needed at the minimum and maximum periods of solar heating. Multichannel SSTs (MCSST) from polar orbiter infrared sensors are the only means presently available to attempt this arduous task.

II. Diurnal Ocean Surface Layer Model

The DOSL model uses the scaling relationships derived by Price et al. (1986) to relate the expected afternoon mixed-layer response to the local atmospheric forcing. A model similar to that of Price et al. (1978) was used to simulate the extensive ocean mixed-layer data set obtained from the R/V *Flip* using rapid-profiling conductivity-temperature-depth and VMCM current meters. These detailed observations and model runs enabled Price et al. (1986) to develop and verify scaling relationships that predict the afternoon SST warming and transient layer depth using surface heat fluxes and surface wind stress values. This parameterization was later verified by Bowers et al. (1986) and Price et al. (1987) with independent data from the northwestern Atlantic.

These scaling relationships are the basis for the DOSL model now functioning in real time with global coverage at FNOC (Clancy, 1986). It forecasts the change in day-night SST (ΔT) and diurnal thermocline depth (D), valid everywhere in the local afternoon. This diurnal SST variation will occur locally from a minimum near 0600 to a maximum about 1400 local time. The change due to diurnal heating is given by Equation 1:

$$\Delta T = 1.5 \frac{(-g\alpha)^{0.5}}{C} \frac{(HPF)^{1.5}}{S}, \quad (1)$$

where g is the acceleration of gravity, α is the expansion coefficient for seawater, C is the heat capacity of seawater, H is the maximum net downward surface heat flux (latent + sensible + infrared + solar) during the day, P is 1/2 the time interval over which the net surface heat flux is downward, S is the wind stress parameter, and F is a radiation extinction function.

The parameter S is calculated from

$$S = \frac{2\tau}{f} [1 - \cos (fP)]^{0.5} , \quad (2)$$

where τ is the surface wind stress averaged over the period of net downward surface heat flux and f is the Coriolis parameter. The radiation function F is derived from

$$F = 1 - \frac{0.4 (2I - H) \exp (-kD)}{I} , \quad (3)$$

where I is the maximum surface solar heat flux during the day and k is the extinction coefficient for solar radiation (Clancy, 1986).

The forcing functions are derived from the Navy Operational Global Atmospheric Prediction System (NOGAPS) model (Rosmond, 1981). This model provides forcing functions on a global, 73 × 144 spherical grid that yields a resolution of 2.5°. These forcing fields are subsequently interpolated to the 63 × 63 polar stereographic grid on which DOSL runs. This latter grid provides resolutions that vary from 200 km (tropics) to nearly 400 km (polar regions). In determining S, the wind-speed-dependent drag coefficient of Garrat (1977) is used to calculate surface wind stresses from the NOGAPS 19.5-m winds. Also, the algorithms of Clancy and Pollak (1983) are used to interpolate the surface heat fluxes and wind stresses between the 6-hourly values provided by NOGAPS (Clancy, 1986).

Particular attention should be paid to the forcing function grid resolution. The subtropical zones with the best chances of strong diurnal heating occur between 20° and 30° from the equator. NOGAPS has a resolution near 275 km and, thus, cannot clearly define mesoscale heating events that may occur and cannot be verified with high-resolution, satellite-derived SSTs. The forcing function spatial definition is, thus, one limiting factor in the DOSL accuracy.

The DOSL model produces a forecast once per day at 00Z (Greenwich Mean Time), which is valid worldwide in the *local* afternoon. This means that the valid DTG (Date-Time-Group) (86081500 is 00Z 15 Aug 86) is a function of longitude. The valid time at a particular location is

$$\text{Time} = DTG + 14 \text{ hr} + \frac{L (1 \text{hr})}{15^\circ}$$

$$\text{for } 0 \le L \le 270^\circ\text{W} \quad (4)$$

and

$$\text{Time} = DTG + 8 \text{ hr} + \frac{(L - 270)}{15^\circ}$$

$$\text{for } 270 \le L \le 360^\circ\text{W} , \quad (5)$$

where L is the longitude of the location ranging from 0° to 360° measured positive westward (W) from Greenwich.

The table illustrates sample valid forecast times at different longitudes for the same DTG of 86081500.

Longitude	L (°W)	Valid DTG (Z)	Local Time
15°W	15°	86081515	1400
75°W	75°	86081519	1400
150°W	150°	86081600	1400
150°E	210°	86081604	1400
60°E	300°	86081510	1400
15°E	345°	86081513	1400

Sample graphical DOSL output (6 August 1987) is shown in Figure 1. The large FNOC chart size and day/night SST difference contours at 0.2°C intervals necessitate exhibiting just the Atlantic and East Pacific basins; otherwise, interpreting values would be quite difficult. One can readily locate areas where significant warming (greater than 1°C) is forecast by the closely bunched contours in numerous regions.

The North Atlantic is particularly active, with greater than 1.5°C warming predicted by the DOSL model for the Gulf of Mexico, the Gulf Stream, the Northeast Atlantic south of Iceland, and the two local maxima at 30°N off Northwest Africa. The number and intensity of changes forecast for 6 August 1987 is not the norm. A scan through weeks of charts reveals that the patterns change dramatically in size, in shape, and in value from one day to the next as the synoptic weather pattern evolves.

Figure 2 illustrates the corresponding surface wind and atmospheric pressure fields (6 August 1986) available from the FNOC marine wind analysis. The 1024-mb subtropical high centered between 20°–30°N stretches across a huge longitudinal range and readily dominates the weather and, thus, cloud cover. This event is a critical factor in that subsidence within the high will tend to deter cloud development, thus opening the way for high insolation. Light winds are also the rule, as evidenced by the lack of wind barbs within the center. (Higher resolution wind fields will be covered later.)

III. Diurnal Warming and SST Measurements

Insolation affects the entire mixed-layer water column to various degrees, depending on several factors: amount of solar heating, surface wind stress, water clarity, and temperature stratification when the heating event first begins. The warming is initially more abrupt at the sea surface and is thus reflected in the

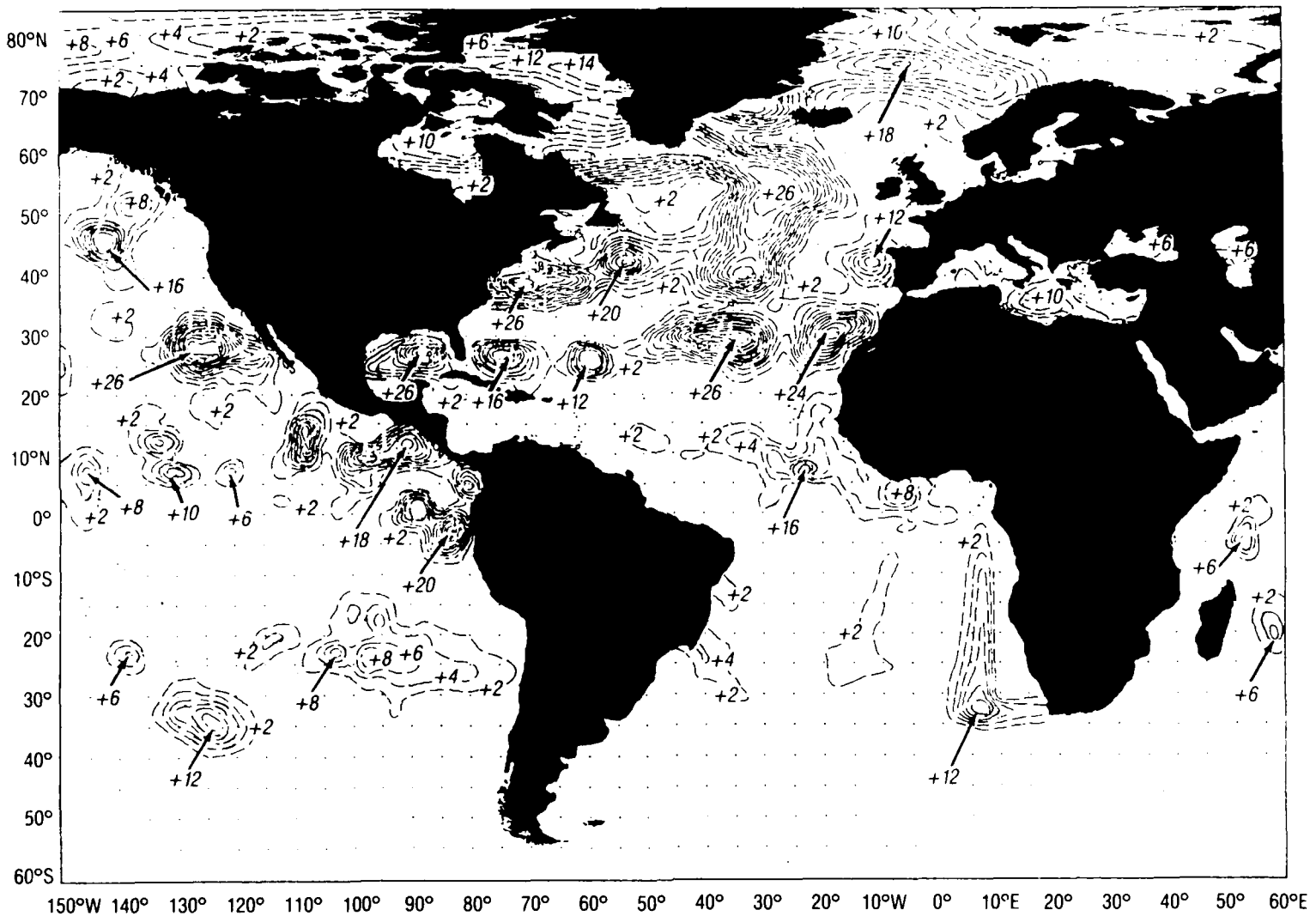

Figure 1. Sample graphical output from the DOSL model for 6 August 1987. Contours every 0.2°C represent forecast of diurnal change in SST valid everywhere at local time of maximum insolation. (Note all chart values should be multiplied by 0.1.)

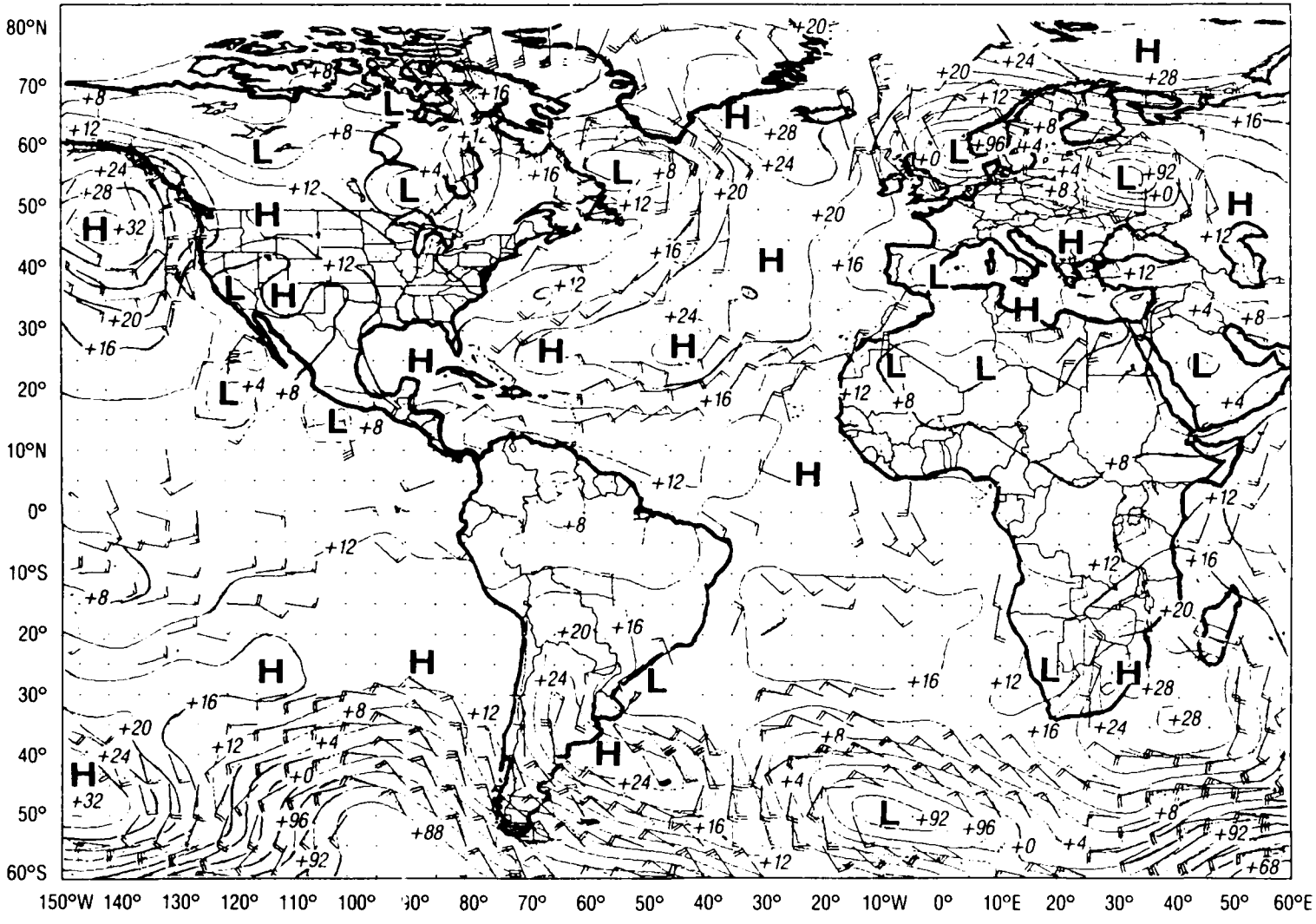

Figure 2. Surface marine wind analysis from FNOC for 1200Z August 6 1986. Isolines represent contours of pressure at 4-mb intervals and define the location of high- and low-pressure systems. Add 1000 mb to all values < 50 and add 900 to all values > 50 to get correct pressure. Wind barbs are plotted every 5° of latitude and longitude in areas of change to show surface wind field. One barb = 10 kt (5 m/s) and one-half barb = 5 kt (~ 2 m/s).

SST as a "hot spot" when compared to surrounding ambient SST values not impacted by the above conditions. As these favorable diurnal warming conditions continue, the mixed layer shallows and warms, creating a stratified layer that may destroy the surface acoustic duct.

This so-called afternoon effect is critical to Navy ASW strategies (Urick, 1983, and Laevastu and Hubert, 1970). Knowledge of when the diurnal warming will negate use of the surface acoustic duct is important for a variety of sensor/weapon applications. The DOSL model could thus be used as one of several tools (along with the Thermodynamic Ocean Prediction System—TOPS) to help locate where the afternoon effect may take place. Appropriate action by naval forces could then lessen the chances that incorrect sensors or sensor deployment patterns were used within the specific domain of interest.

Intense diurnal warming may create sharp, horizontal SST gradients that could be readily confused with other features related to real mesoscale ocean frontal boundaries. The generation of these gradients is especially disconcerting, since the regional FNOC three-dimensional thermal structure analyses (Optimum Thermal Interpolation System—OTIS) are gradually becoming more dependent on frontal "boguses" derived by analysts who extract frontal locations and strengths from infrared imagery. Thus, misleading SST gradient information could be passed onto the OTIS analysis if diurnal warming events are not screened out.

Observations of sea surface warming due to insolation (diurnal heating) have been inadequate for many years (Cornillon and Stramma, 1985). Ship weather reports include SST readings that are often representative of the engine intake temperatures (Earle, 1985). As such, they occur well below the water line (sometimes as deep as 15-20 m) and, thus, do not indicate the true SST. Some researchers have argued that this aspect is a positive factor and surface skin effects are negated, and that the ship values are a measure of the "mixed-layer" temperature.

This logic does not hold true when dealing with the topic of diurnal surface heating. Surface heat fluxes and wind stress are the key to determining whether large temperature changes will occur at the ocean surface on a daily time scale. Therefore, the skin temperature (the apparent temperature of the sea that is in contact with the air) is the critical sea measurement, not some temperature value at a depth of 5 m or 10 m. This fact significantly raises the value of satellite infrared SSTs for the study discussed here.

IV. Satellite-Derived Sea Surface Temperatures

Satellite-derived SSTs have progressed significantly since the first infrared sensors were used. Meteorological applications paved the way for the first series of environmental satellites, but oceanography was a distant by-product due in part to poor thermal sensitivity. This restriction was lifted when the TIROS-N series of National Oceanic and Atmospheric Administration (NOAA) polar orbiters began using 10-bit digitization (0.12 °C sensitivity) over the whole range of possible SSTs. Small SST gradients could then be viewed and surface currents mapped as never before possible. However, the use of single-channel infrared data is limited by the attenuating effect of atmospheric water vapor. Maul (1983) clearly states the debilitating effect water vapor can have by calculating potential SST corrections ranging from nearly 0 to as much as 10°C. These values are truly disconcerting when realizing that such errors can immediately rule out the vast majority of studies that rely on absolute SST values for quantitative studies.

In 1981, NOAA began the operational production of MCSSTs by using the differential absorption observed in two infrared channels. The 10.3-11.3μm and 11.5-12.5μm channels were used to generate a correction value applied to the 11.5-12.5μm value that removed the major water vapor effects. Thus, the differing response between the two infrared spectral bands to the same columnar water vapor permitted the calculation of a correction factor, which fluctuates as the water vapor varies.

The NOAA Advanced Very High Resolution Radiometer (AVHRR) is now a five-channel sensor that includes an additional spectral band between 3.5μm and 3.93μm. This addition enables the use of a three-channel algorithm that can be superior to the two-channel, split-window equations (channels 4 and 5) when the ever-present noise in channel 3 is low just after launch or satellite outgassing. This problem will be corrected for the NOAA K,L,M series by incorporating slightly different sensor technology.

The MCSST allows the adjustment to be done on a pixel-by-pixel basis and eliminates the need for additional data sources, such as atmospheric sounders, which are plagued with poor spatial resolution or radiosondes that provide sparse coverage over ocean domains. NOAA processes global area coverage (GAC) 4-km data in 2 × 2 unit arrays to produce 8-km MCSSTs on a daily basis. The procedure to create MCSSTs has been refined over the years, and their accuracy has continually increased to the point where they now have an RMS error of 0.6-0.7°C (Strong and McClain, 1985) while producing 70,000 to 100,000 global retrievals per day. This measurement milestone allows MCSST usage for a wide variety of research and operational projects.

These National Environmental Satellite, Data, Information Service (NESDIS) MCSSTs are processed orbit by orbit as the GAC data are downloaded from the spacecraft tape recorders. The time delay from sensor data collection to MCSST retrieval residing in

the NESDIS current day observation file varies from 3 to 6 hours. These data can then be accessed by operational activities and incorporated into SST or three-dimensional ocean thermal analyses.

This processing procedure is designed to create a reasonable global distribution to satisfy a variety of SST mapping requirements. However, not all cloud-free pixels are used to generate MCSSTs. The MCSST algorithm incorporates a search pattern that finds 1 (low), 5 (medium) or 15 (high) observations per 11 × 11 GAC array (about 50 × 50 km). This factor limits the total number of MCSSTs produced and results mainly from several considerations—disk space, processing time, and overall data needs. Thus, hundreds of thousands of potential MCSST retrievals are not produced each day.

The DOSL validation effort could use isolated matchups between day/night MCSST measurements and DOSL model output but is unrealistic for several reasons: no DOSL digital values were retained, only the contoured charts; interpolating coarse DOSL values to MCSST locations may induce large errors; and this method would not permit us to see whether the pattern of diurnal heating was being correctly reproduced. Therefore, MCSSTs (imagery) provides us with the synoptic scale coverage and highly accurate SST values required for DOSL comparisons.

V. Validation Technique

Cloud contamination severely restricts any validation effort that relies solely on infrared imagery. Therefore, instead of acquiring images in real time, the project relied on the DOSL model to indicate which regions should be viewed more closely. The first phase revolved around the collection of FNOC's DOSL and marine surface wind charts for the 1986 Northern Hemisphere summer months. The charts were subjectively scanned to select only events that exhibited large diurnal warming over a spatial domain greater than 10° longitude (approximately 1000 km).

DOSL charts for August, September, and most of October 1986 were scrutinized to find likely maximum diurnal heating events that would probably be associated with few clouds and thus indicate very good infrared imagery viewing conditions. Dozens of cases were located in the North Atlantic, the Mediterranean Sea, and the central and eastern North Pacific, as well as a few isolated occurrences in other spots. These potential case studies were then screened by taking into account the conditions usually found in each area.

The North Pacific is well known for the extensive cloud coverage generated by the combined effects of the meteorological and oceanographic conditions that are manifested through air-sea interaction processes. These conditions are prevalent in the summer and the late fall when visible or infrared viewing is extremely poor at best. However, the DOSL model predicted large diurnal warming based on the forecast of light winds and little surface mixing even though skies were cloudy. The North Pacific was eliminated from further study, since the infrared data were not suitable.

The Mediterranean Sea was initially thought to be a superior location for testing the DOSL model, but several problems arose. Excellent satellite viewing is the rule rather than the exception and permits regular infrared surveys. Light winds and insolation can quite frequently cause the model to forecast diurnal heating of 2°C. However, the regions of heating can be small, are quick to dissipate and reappear, and are difficult to time with regards to satellite overpasses. The region also frequently contains dust and aerosols, which can attenuate infrared signals and decrease the accuracy of measurements.

Earlier efforts by Cornillon and Stramma (1985) and Stramma et al. (1986) showed that selected regions in the Sargasso Sea experienced diurnal warming in excess of 1°C up to 30 percent of the time. DOSL charts were checked to locate days when significant heating was forecast and then nearly 100 NOAA AVHRR digital images were scrutinized to find cloud-free, day/night image pairs. These data were previously collected in real time by the NORDA Satellite Digital Receiving and Processing System (Hawkins et al., 1985) to support the GEOSAT Ocean Application Program (GOAP; Lybanon et al., 1987). GOAP combined the synoptic infrared coverage with precision GEOSAT altimeter sea surface height data to map mesoscale front and eddy features within the Gulf Stream system. All data were high picture resolution transmission data (1 km) from either Wallops Island, VA, or the NORDA tracking antenna.

The DOSL model output indicated numerous cases where warming larger than 1°C should have been visible in satellite imagery. However, a quick look at the digital images revealed very few suitable cloud-free pairs. Many day/night MCSST difference images were generated, but none were of sufficient quality for this study, even though cloud-free bits and pieces did verify well with DOSL values.

Attention was then turned to the central and eastern North Atlantic, since the Azores-Bermuda high was often creating good cloud-free conditions. These conditions were evident in the persistently high DOSL diurnal heating forecasts. Numerous AVHRR digital images were ordered from NESDIS for further investigation. Both 1-km local area coverage and 4-km GAC data were included to see whether or not one was preferable to the other (note that Cornillon and Stramma, 1985, found 4 km sufficient for their study). Imagery for 16-18 and 28 August; 3, 15, 23, and 30 September; and 2 and 7 October 1986 were then read in and initially scanned for cloud contamination. A quick survey concluded the August data were far superior, and they were then processed further.

The small number of cases were deemed insufficient in quantity, so attention was turned to other methods to increase the case study comparisons. Lessons learned during the 1986 summer were then incorporated into a near-real-time effort in the 1987 summer. DOSL charts were checked daily in the North Atlantic to try and catch the beginning of diurnal heating events. Conditions normally changed in logical phases as cloud systems with higher winds moved out and were followed by clearer skies and weaker winds. Direct communication between FNOC and NORDA personnel permitted the collection of several more cases. Each example, whether for 1986 or 1987, was processed in the following manner:

- NOAA-9 channels 4 and 5 data were calibrated and earth-located using software on NORDA's Interactive Digital Satellite Image Processing System (IDSIPS; Hawkins et al., 1985).
- Earth location was fine-tuned using European, African, and island landmarks and resulted in registration accuracies of 2 pixels or better.
- Channels 4 and 5 were used for both day and night passes instead of 3,4,5 for the night and 4,5 for the day to be consistent and to reduce the introduction of noise inherent in channel 3. Conservative cloud tests were incorporated that likely erred on the side of eliminating some cloud-free pixels to make sure partially cloudy pixels were not allowed to slip through and introduce erroneous data points in the final results.
- Multichannel split-window SSTs were calculated for all cloud-free pixels in both day and night imagery using the NESDIS operational equations valid for the period (Strong and McClain, 1985).
- Daytime MCSST imagery was then subtracted from the nighttime versions to produce a day/night difference image. These imagery were then falsely colored in 0.5°C increments to view more easily the regions of maximum diurnal heating. Clouds were masked in black or dark gray.

The DOSL charts were not, however, in an easy format to compare directly with the images. Thus, the charts were digitized on IDSIPS and processed to the exact image map projection and scale. Isotherm contours at 0.2°, 0.5°, 1.0°, 1.5°, 2.0°, and 2.5°C were kept and all others were interactively erased to reduce the cluttered pattern in intense heating regions (DOSL output originally contains contours at 0.2°C intervals). DOSL contours could then be directly overlaid in a graphics plane on top of the falsely colored, day/night difference images.

VI. Validation Results

August 1986 was an excellent diurnal heating event time due to the meteorological conditions that existed in the central and eastern North Atlantic. The subtropical high dominated the central North Atlantic and contained vast areas of subsidence, as evidenced in pressure maps, such as shown in Figure 2. Infrared imagery was relatively cloud-free for a large region bounded by 25-40°N and 10-45°W.

A. 16 August 1986

Figure 3 (1537Z 16 August 1986) is dominated by a warm, dark-red patch of SSTs oriented northeast to southwest off the extreme northwestern African coast. This section of very warm SSTs extends westward over 20° longitude and is cloudless in the most intense area near 31°N and 16°W. This very warm water is in direct contrast to the much cooler coastal upwelling along the northeastern African coast and contributes to a substantial SST gradient.

The day/night MCSST image (Fig. 4) readily illustrates the scale of the diurnal heating taking place. A huge area of SST warming ranges from 0.0° to 0.5°C and covers a section surrounding the zone of maximum warming. A light-blue color was purposely chosen to offset it from the black and dark-gray shades used for cloud-contaminated pixels. This coloration permits the viewer easy visual access to the image content. (Note that there is little fading from one color to another in the color wedge, especially between 1° and 6°C, required to enhance each 1.0°C day/night temperature warming bin).

Close examination is needed to spot diurnal heating from 1.0° to 2.0°C, even though it has been colored dark-blue to offset it from the previous light-blue color and the following dark-green (2.0° to 3.0°C) shade. This 1°C bin is scattered about the image but is usually concentrated near the maximum heating sections.

The 3.0° to 5.0°C diurnal heating bins (yellow and orange) are concentrated in limited sections and nicely outline regions of even higher heating. These values typically fall between 25° and 35°N and cover virtually the whole longitudinal range. This example of diurnal heating is impressive, even without the larger values found within the yellow- and orange-colored pixels. Note that conservative cloud tests were applied to ensure that few clouds contaminated the day/night images. Thus, some of the dark gray pixels located near 32°N and 23°W may actually be cloud-free or partially cloudy, but were masked out so that a simple test could be applied to the entire image.

The DOSL contours (valid for the afternoon of the 16th and overlain in white in Fig. 4) outline the general diurnal heating pattern. The very abrupt zone of heating just off the coast is well covered with a DOSL contour in excess of 1.0°C. The model forecast correctly predicts warming to occur around 25°N across a wide ocean expanse. Two large pockets of 2.5°C warming occur at 26°N, 25°W and at 32°N, 35°W in the DOSL product, where the westernmost area agrees well with the day/night MCSST imagery. The eastern maximum is slightly misplaced to the southeast.

Figure 3. MCSST image at 1537Z 16 August 1986 reveals extremely hot SST values off NW African coast. Clouds have been blacked out using a multichannel cloud-screening technique. SSTs have been falsely colored according to temperature scale in upper-right corner. Note patch in excess of 26°C near 31°N, 16°W.

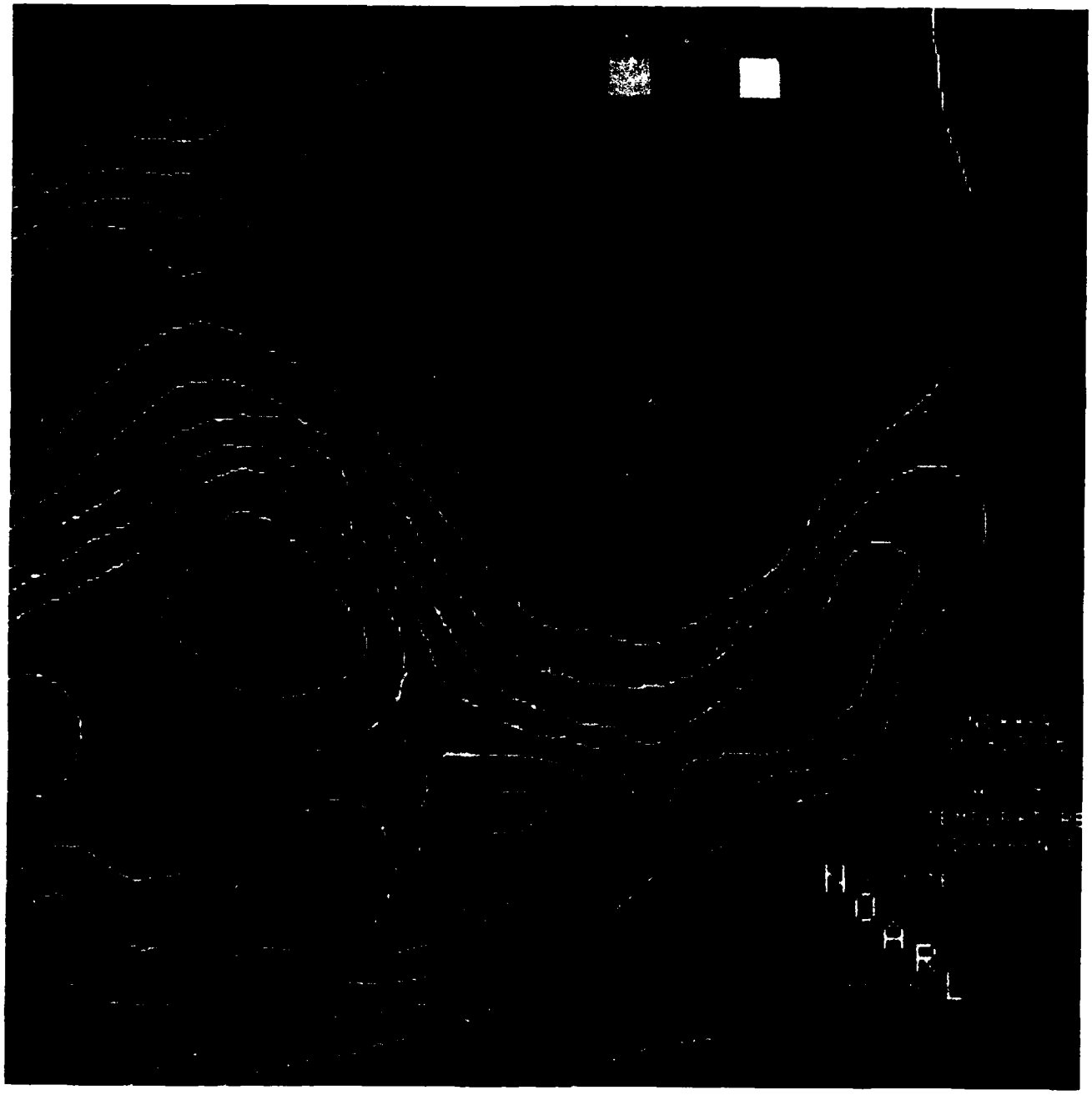

Figure 4. The 16 August 1986 day-night MCSST difference image, color coded according to temperature scale in 0.5°C and 1.0°C increments. Light blue represents diurnal increases near 1°C; yellow is near 3°C. White contours are FNOC DOSL SST change forecast values at 0.2°C intervals. Note how well elongated region off NW Africa correlates with DOSL local maximum.

The trend exhibited in Figure 4 represents excellent agreement between the DOSL output and the day/night MCSST imagery when considering the heating pattern. This agreement indicates that the wind stress and the surface heat fluxes are being correctly forecast by NOGAPS in terms of the overall meteorological conditions and are incorporated correctly by the DOSL model's physics. The few regions of very intense heating, dramatically shown in imagery, reveal that the 2.5°C upper bound within the DOSL model can be a limiting factor in certain cases. This threshold exists, since the model physics begin to break down for values above 2.5°C.

One should also note the grid-point resolution involved in the input fields. NOGAPS has 2.5° spacing and is extremely mismatched when confronted with the realities of 1-km or 4-km imagery. Thus, the smoothing of heating effects is to be expected and will continue to be the norm until the atmospheric forcing and the DOSL model grid resolution are significantly reduced. In this light, the model appears to do quite well by mapping out the prime diurnal heating spots.

B. 17 August 1986

The following day, 17 August, also exhibited similar diurnal warming features, but not with quite the widespread intensity evident on August 16. Figure 5 shows a large east-west section of DOSL-predicted afternoon warming that closely agrees with the 0.0°-0.5°C (light blue) MCSST day/night difference. The eastern segment is not quite as sharply defined as in the previous day, but some cloud-free pixels have likely been masked out due to high surface reflectivity values caused by sunglint near 30°N, 15°W.

The DOSL maximums near 30°N, 18°W and 33°N, 32°W are somewhat cloudy; thus, good comparisons are difficult. However, the imagery clearly indicates several zones of 3° and 4°C heating between the two westernmost DOSL warming areas. Thus, the overall trend appears to be correct, but individual locations are hard to verify due to spotty cloud contamination.

It should be noted that although the DOSL model has a 2.5°C threshold, the day/night MCSST maximum values of 3°-4°C compare well with the earlier results of Cornillon and Stramma (1985) in the Sargasso Sea. Both areas are affected by the fringe of the Azores-Bermuda high, but on opposite sides. The eastern North Atlantic has the advantage that no major current system with large SST signals runs through the area. The Gulf Stream forces investigators to move to the south, away from the disturbing changes that can occur due to the energetic Gulf Stream cold-core rings.

C. 6 August 1987

This example involves a situation in the central North Atlantic using NORDA-acquired, 4-km GAC data. Figure 6 shows the data at about 4 km resolution (considerably better than previous cases) and permits us to focus on a zone within the Azores-Bermuda high. A pronounced region of 0.0°-0.5°C warming is outlined in light blue and agrees well with DOSL contours in shape and extent. More importantly, the main area of intense heating falls well within the 2.0°-2.5°C DOSL values.

Diurnal heating values of 3°-4°C align along 29°-30°N and 30°-45°W. These numbers exceed the DOSL threshold (as in the previous cases), but speak well for the model, considering the resolution for input forcing functions. The fact that clouds lie to either side the maximum warming indicates that NOGAPS appears to have done well in forecasting the meteorological conditions. The extra region of high values in Figure 6 suggests that NOGAPS is in error. A band of clouds oriented northeast-southwest separates the two high-value sections, but DOSL misses the northwestern segment by labeling it as 0.2°-0.5°C instead of the 2°-4°C heating present in the imagery.

The corresponding surface winds at 00Z 6 August 1987 are outlined in the FNOC Marine Wind Analysis (Fig. 7). This analysis is separate from the NOGAPS fields and includes a combination of ship-, island-, and satellite-derived wind retrievals. Isobars at 4-millibar (mb) contour intervals are superimposed with high- (H) and low- (L) pressure centers and with vectors (half barb = 5 kt, full barb = 10 kt, etc.).

As expected, the Bermuda High dominates the meteorological pattern throughout most of the North Atlantic from 25°N-35°N. Winds near 15-20 kt surround the region, but much calmer conditions reside in the high-pressure center as warm, dry air subsides from above. This situation helps to reduce tropical cloud development and promotes diurnal heating.

These light winds are also verified by the Special Sensor Microwave/Imager (SSM/I) launched June 1987 aboard a Defense Meteorological Satellite Program spacecraft. This passive microwave sensor is similar in frequency and purpose to the Nimbus-7 scanning multichannel microwave radiometer, but has finer spatial resolution (25 km) and better on-board calibration. It can measure surface wind speed (2 m/s), columnar water vapor (0.3 g/cm^2), and sea-ice concentration (10 percent), among other parameters (Hollinger, 1989).

The SSM/I can measure surface winds in essentially all weather conditions. Heavy rain cells can cause erroneous retrievals, but these values can be detected by flagging regions of heavy precipitation, another parameter sensed by the SSM/I. The 1394-km SSM/I swath permits wide sector viewing during its 14 polar orbits. However, data gaps exist below 50°, since consecutive passes do not overlap. The gap increases to 1000 km at the equator and is then filled in largely by orbital data 12 hours later. Complete global coverage occurs every 36 hours.

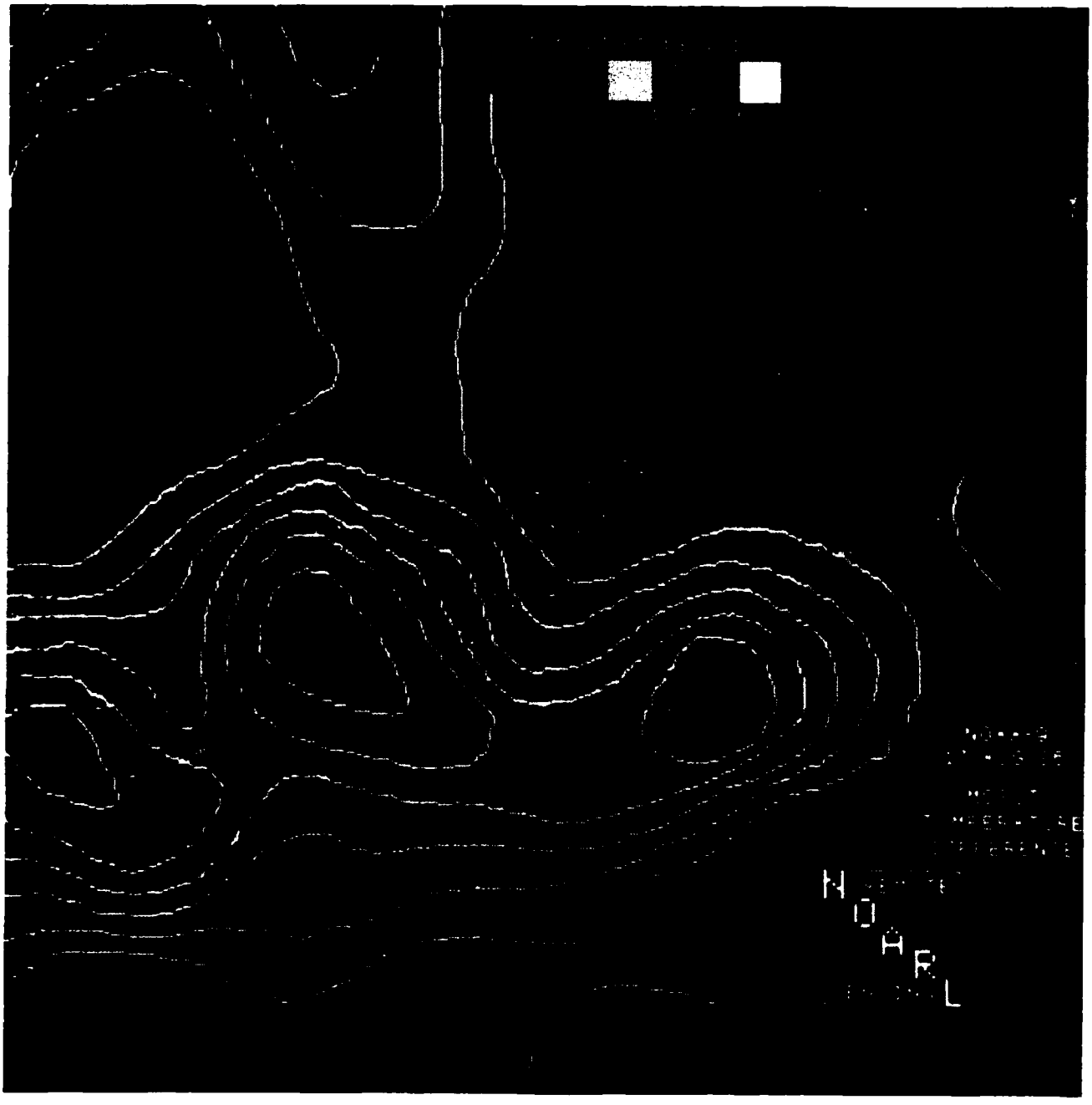

Figure 5. The 17 August 1986 day-night MCSST difference image, color coded according to temperature scale. General agreement in western portion, but DOSL values are too high in area of previous maximum, as seen in Fig. 4.

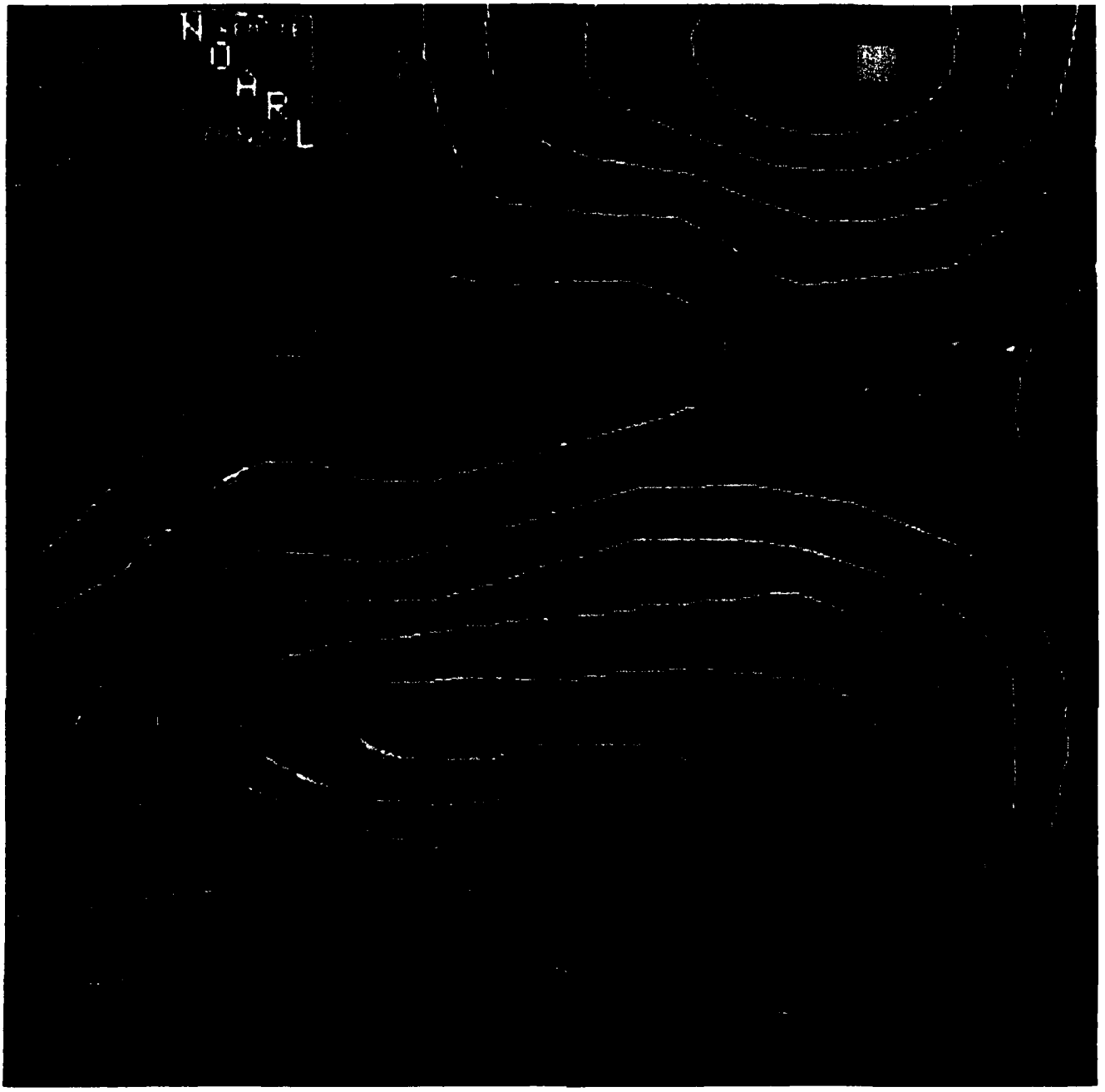

Figure 6. The 6 August 1987 day-night MCSST difference image, color coded according to temperature scale. This image focuses on area near center of subtropical high to reveal intense diurnal heating in excess of 4°C, but is well mapped by the DOSL contours. Note this figure uses higher spatial resolution than incorporated in Figs. 4 and 5.

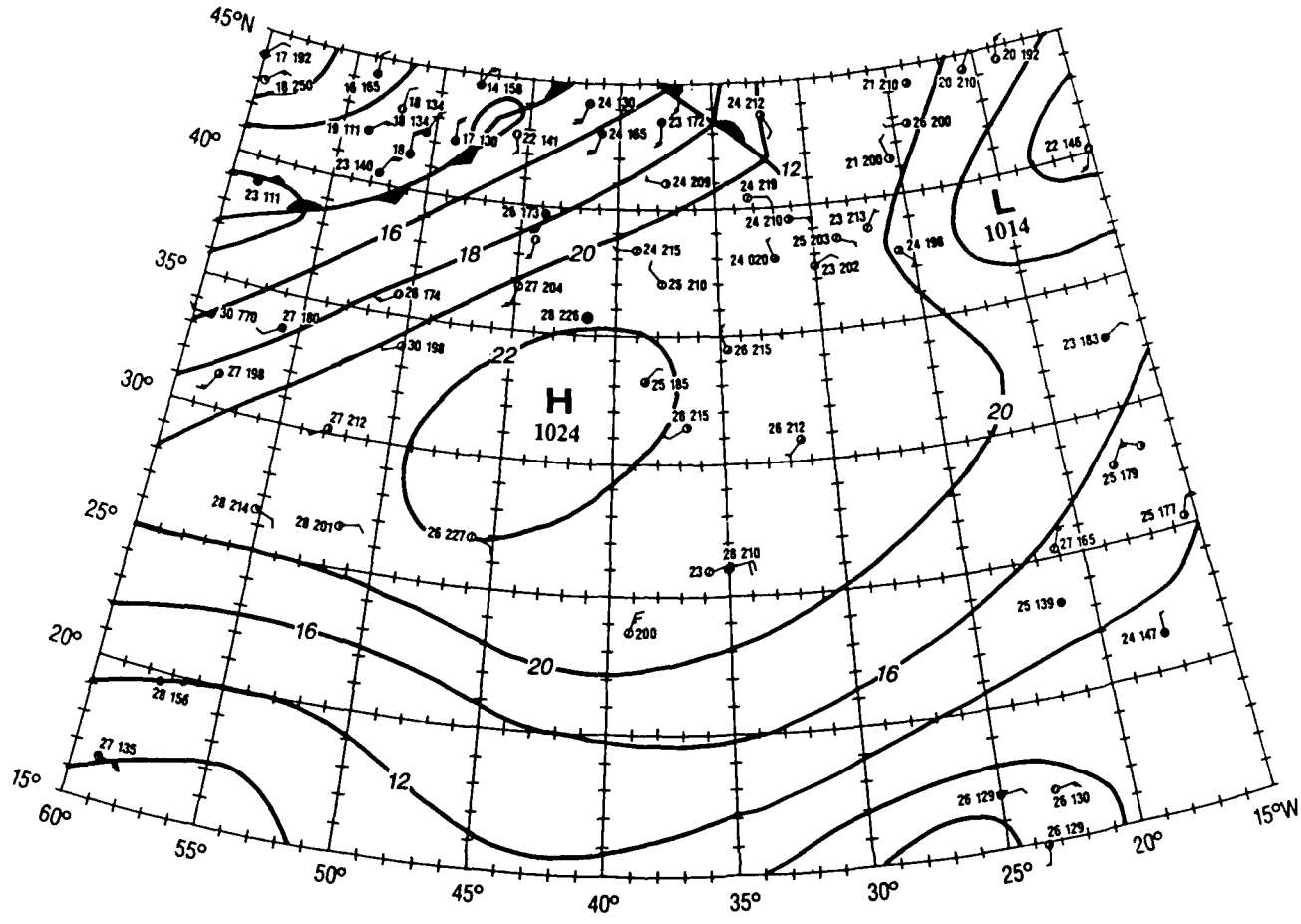

Figure 7. NOAA National Hurricane Center surface weather analysis for 1200Z 16 August 1986. Pressure contours at 4-mb intervals; wind vectors of one-half barb = 5 kt (~ 2 m/s) and one barb = 10 kt (5 m/s). The two sets of numbers next to each ship weather observation are air temperature (°C) and surface pressure (multiply value by 0.1 and add 1000 mb to get correct value). Sky cover is marked by the black portion of observation circle (i.e., open circle with a line denotes no clouds, half a black circle indicates presence of 50% clear skies). Note clear skies in center of subtropical high near 30°N, 40°W.

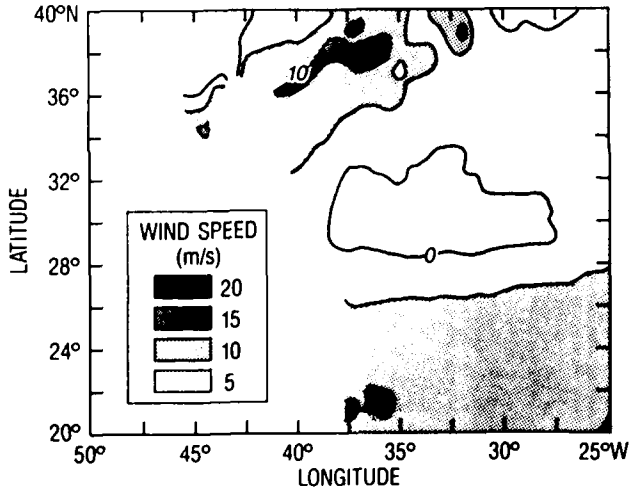

Figure 8. SSM/I surface winds on 6 August 1987 for 0700Z to 1000Z. The 25-km wind retrievals have been mapped into a two-dimensional field to examine the general wind speed patterns. A large zone of winds less than 10 kt (5 m/s) parallels 30°N.

Figure 8 represents several passes covering the DOSL image domain for 5 August 1987 (no SSM/I values available on 6 August due to satellite coverage gaps). The wind speed retrievals are contoured at 5-m/s intervals and are shaded to help the viewer easily recognize the zones of constant wind speed. Light winds dominate the region and provide accurate backup information to the marine wind analysis.

VII. Future Considerations

The NOGAPS model has undergone considerable revision since 1987 and now contains an entirely new treatment for the atmospheric boundary layer. The new approach has proven to be far superior to the earlier version, so heat fluxes for DOSL input have been upgraded significantly since this study began.

The NOGAPS and DOSL spatial resolution of 2.5° is quite coarse when attempting to nail down diurnal heating features that can be very localized.

Future reductions in model grid spacing will help to solve this problem.

Sampling day and night SSTs to validate DOSL results with one polar orbiter is difficult. Any follow-on studies should seriously consider the use of geostationary data that provide views every 30 minutes and that remedy some of the cloud contamination problems caused by compositing over short intervals as clouds move. The critical element is the accuracy of SSTs from the Geostationary Operational Environmental Satellites (GOES). The VISSR Atmospheric Sounder has reached accuracies of less than 1°C, but improvements are needed before it is equivalent to MCSSTs. This will likely come about with GOES-NEXT in 1990-91, where multi-infrared channels and 10-bit digitization will open up more applications for these platforms.

VIII. Summary and Conclusions

As shown by the work of Cornillon and Stramma (1985), Stramma et al. (1986), and many others, diurnal SST variability is ubiquitous and widespread during the spring and summer. Forced by day/night variations in the net surface heat flux and strongly modulated by the magnitude of the surface wind stress, this phenomenon dominates short-term variability in upper-ocean thermal stratification (Price et al., 1986), and thus critically impacts on surface-duct acoustics.

Diurnal SST variability is also important when using and interpreting satellite SST data. Satellites measure the skin temperature of the ocean, which may or may not be characteristic of the average temperature above the seasonal thermocline, depending on the amplitude and phase of the diurnal SST cycle at the time of measurement. Furthermore, because the diurnal SST response is such a strongly nonlinear function of the wind speed, smoothly varying patterns of the synoptic wind field tend to produce sharp horizontal gradients in diurnal SST features, as demonstrated by the satellite imagery presented here. These sharp horizontal gradients would be easy to misinterpret as water mass boundaries.

Price et al. (1986) developed scaling relationships relating the amplitude of the upper ocean's diurnal response to wind-stress and heat-flux parameters. They verified these relationships, referred to as the DOSL formulation, by using observed winds, heat fluxes, and SSTs at a moored buoy.

Results from a real-time synoptic implementation of the DOSL model at FNOC were presented and the predictions of this model were verified with satellite MCSST data. The case studies discussed here were biased to the extremely warm diurnal heating events, since the infrared imagery must obviously be cloud-free for use and, thus, large-magnitude diurnal heating has an increased chance to occur. The DOSL correctly defined the shape or pattern of each heated region, but the upper bound on the warming is too low by virtue of the self-imposed upper bound of 2.5°C. Day/night MCSST differences reached 3°-5°C in several cases when light winds combined with intense summertime insolation in the subtropical highs.

IX. Recommendation

DOSL has proven to handle these extreme cases well in a qualitative manner and thus can be used for several immediate applications. This report recommends that the DOSL model be declared operational and used to fill the gap existing in forecasting daily SST diurnal warming events.

X. References

Bowers, C. M., J. F. Price, R. A. Weller, and M. G. Briscoe (1986). *Data Tabulations and Analysis of Diurnal Sea Surface Temperature Variability Observed at LOTUS.* Woods Hole Oceanographic Institution, Woods Hole, MA. Technical Report WHOI-86-5, 54 pp.

Clancy, R. M. and K. D. Pollak (1983). A real time synoptic ocean thermal analysis/forecast system. *Progress in Oceanography* 12:383-424.

Clancy, R. M. (1986). *Technical Description of the Diurnal Ocean Surface Layer (DOSL) Model.* Fleet Numerical Oceanography Center, Technical Note 422-86-01, 8 pp.

Cornillon, P. and L. Stramma (1985). The distribution of diurnal sea surface warming events in the western Sargasso Sea. *Journal of Geophysical Research* 90(C6):11811-11815.

Earle, M. D. (1985). *Statistical Comparisons of Ship and Buoy Marine Observations.* MEC Systems Corp., 10629 Crestwood Dr., Manassas, VA 22110, Report MEC-85-8.

Hawkins, J. D., et al. (1985). NORDA remote sensing, EOS oceanography report. *Transactions of the American Geophysical Union* 66(23):482-483.

Hollinger, J. (1989). *DMSP SSMI Calibration/ Validation Final Review.* Naval Research Laboratory, Washington, DC, 159 pp.

Laevastu, T. and W. E. Hubert (1970). *The Effects of "Transient" Thermoclines on ASW Operations.* Fleet Numerical Oceanography Center Technical Memo No. 26, 11 pp.

Lybanon, M. and R. L. Crout (1987). The NORDA GEOSAT ocean application program. Johns Hopkins University, *APL Tech Digest* 8(2):212-218.

Maul, G. (1983). Zenith angle effects in multispectral infrared sea surface remote sensing. *Remote Sensing of Environment* 13(5):439-451.

McClain, E. P. (1981). Split window and triple window sea surface temperature determinations from

satellite measurements. *1981 ICEX Statutory Meeting,* 6-10 October.

McClain, E. P., W. G. Pichel, and C. C. Walton (1985). Comparative performance of AVHRR-based multichannel sea surface temperatures. *Journal of Geophysical Research* 90(6):11587-11601.

NOAA/NESDIS. Coefficients presented at the 40th SST Research Panel Meeting, National Environmental Satellite, Data, and Information Service, National Oceanic and Atmospheric Administration, Suitland, MD, July.

Price, J. F., C. N. K. Mooers, and J. C. Van Leer (1978). Observation and simulation of storm-induced mixed-layer deepening. *Journal of Physical Oceanography* 8:582-599.

Price, J. F., R. A. Weller, and R. Pinkel (1986). Diurnal cycling: observations and models of the upper ocean response to diurnal heating, cooling and wind mixing. *Journal of Geophysical Research* 91:8411-8427.

Price, J. F., R. A. Weller, C. M. Bowers, and M. G. Briscoe (1987). Diurnal response of sea surface temperature observed at the long term upper ocean study (34°N, 70°W) in the Sargasso Sea. *Journal of Geophysical Research* 92:14480-14490.

Rosmond, T. E. (1981). NOGAPS: Navy Operational Global Atmospheric Prediction System. *Preprint Volume, Fifth Conference on Numerical Weather Prediction,* Monterey, CA. Published by the American Meteorological Society, Boston, MA, p. 74-79.

Stramma, L., P. Cornillon, R. A. Weller, J. F. Price, and M. G. Briscoe (1986). Large diurnal sea surface temperature variability: Satellite and in situ measurements. *Journal of Physical Oceanography* 16(5):827-837.

Strong, A. and P. McClain (1985). Improved ocean surface temperature from space—Comparison with drifting buoys. *Bulletin of the American Meteorological Society* 65:138-142.

Urick, R. J. (1983). *Principles of Underwater Sound* (3rd Edition). New York, McGraw-Hill.

Distribution List

Applied Physics Laboratory
Johns Hopkins University
John Hopkins Road
Laurel MD 20707
Attn: Dr. J. Apel

Applied Physics Laboratory
University of Washington
1013 NE 40th St.
Seattle WA 98105

Applied Research Laboratory
Pennsylvania State University
P.O. Box 30
State College PA 16801

Applied Research Laboratory
University of Texas at Austin
P.O. Box 8029
Austin TX 78713-8029

Assistant Secretary of the Navy
Research, Engineering & Systems
Washington DC 20350-2000

Cal Space
5360 Bothe Ave.
San Diego CA 92122
Attn: Dr. R. Bernstein

Chief of Naval Operations
Washington DC 20350-2000
Attn: OP-71
OP-987

Chief of Naval Operations
Oceanographer of the Navy
Washington DC 20392-1800
Attn: OP-096, Malay

CIMAS
4600 Rickenbacker Causeway
Virginia Key FL 33149
Attn: Director

David W. Taylor Naval Research Cntr
Bethesda MD 20084-5000
Attn: Commander

Defense Mapping Agency
Systems Center
12100 Sunset Hill Rd. #200
Reston VA 22090-3207
Attn: Director
Code SGWN

Director of Navy Laboratories
Crystal Plaza #5, Rm. 1062
Washington DC 20360

Fleet Antisub Warfare Tng Ctr-Atl
Naval Station
Norfolk VA 23511-6495

Fleet Numerical Oceanography Center
Monterey CA 93943-5005
Attn: Commanding Officer
Code 40, LCDR D. Steiner
Code 40B, Mr. L. Clark
Code 42, Mr. R. M. Clancy
Code 42, Dr. J. Cummings
Code 42, Mr. K. Pollak
Code 43, Mr. J. Cornelius
Code 70B, Ms. P. Chavasant

Florida State University
MS B-174, 012 LOV
Tallahassee FL 32306-3041
Attn: Dr. J. O'Brien

GFDL-NOAA
P.O. Box 308
Princeton University
Princeton NJ 08542
Attn: Ms. B. Samuels

Harvard University
Division of Applied Sciences
28 Oxford St.
Cambridge MA 02138
Attn: Dr. A. Robinson
Dr. S. Glenn

Institute for Naval Oceanography
Stennis Space Center MS 39529
Attn: Dr. J. Leese
Dr. L. Kantha

Martin Marietta
FNOC Code 40
Monterey CA 93943
Attn: Dr. P. May
Mr. M. Ignaszewski

National Aeronautics & Space Administration
Goddard Space Flight Center
Greenbelt MD 20771
Attn: Code 671, Dr. T. Busalacchi

National Aeronautics & Space Administration HQ
Washington DC 20233
Attn: Dr. E. Njoku

National Meteorological Center
World Weather Building
Washington DC 20233
Attn: W/NMC2, Dr. G. DiMego
W/NMC3, Dr. C. Dey
W/NMC21, Dr. L. Breaker
W/NMC21, Mr. B. Gemmill

National Ocean Data Center
1825 Connecticut Ave., NW
Universal Bldg. South, Rm. 406
Washington DC 20235
Attn: Mr. G. Withee

National Oceanic & Atmospheric Administration
NESS S/RE13, World Weather Building
Washington DC 20233
Attn: Dr. P. S. Deleonibus

National Ocean Survey
Ocean Products Div., WWB, Rm. 201
5200 Auth Rd.
Camp Springs MD 20746
Attn: Mr. R. Barazotto
Dr. W. Campbell

National Ocean Survey
Ocean Applications, Bldg. 4
Fleet Numerical Oceanography Center
Monterey CA 93943-5005
Attn: Dr. M. Holl

National Space Science Data Center
4400 Forbes Blvd.
Lanham MD 20706
Attn: Ms. M. James

National Weather Service
Wx1, GRAMAX
8060 13th St.
Silver Spring MD 23910
Attn: Dr. R. McPherson

Naval Air Development Center
Warminster PA 18974-5000
Attn: Commander

Naval Air Systems Command HQ
Washington DC 20361-0001
Attn: Commander

Naval Civil Engineering Laboratory
Port Hueneme CA 93043
Attn: Commanding Officer

Naval Coastal Systems Center
Panama City FL 32407-5000
Attn: Commanding Officer

Naval Eastern Oceanography Center
McAdie Bldg., U-117
NAS Norfolk VA 23511-5399
Attn: Mr. C. Weigand

Naval Facilities Engineering Command HQ
200 Stovall St.
Alexandria VA 22332-2300
Attn: Commander

Naval Oceanographic Office
Stennis Space Center MS 39529
Attn: Commanding Officer
Code OS, Mr. L. Bernard
Code OS, Mr. M. Boston
Code OST, Mr. A. Johnson
Code OST, Mr. J. Rigney
Code OSTM, Dr. C. Horton
Code OSTM, Mr. R. Rhodes

Naval Oceanography Command
Stennis Space Center MS 39529
Attn: Commander

Naval Oceanographic & Atmospheric Research Laboratory
Stennis Space Center MS 39529-5004
Attn: Code 100
Code 105
Code 110
Code 115
Code 125L (10)
Code 125P
Code 200
Code 222, Mr. G. Kerr
Code 300
Code 321, Mr. D. May
Code 321, Mr. A. Pressman
Code 322, Dr. J. Harding
Code 322, Dr. M. Carnes
Code 322, Dr. T. Bennett
Code 323, Dr. G. Heburn
Code 331, Dr. J. Boyd
Code 400
Code 431, Dr. J. Goerss
Code 432, Dr. T. Rosmond
Code 440, Dr. S. Payne
Code 441, Mr. B. Fett

Naval Oceanographic & Atmospheric Research Laboratory
Liaison Office
Crystal Plaza #5, Rm. 802
Arlington VA 22202-5000
Attn: Mr. B. Farquhar

Naval Ocean Systems Center
San Diego CA 92152-5000
Attn: Commander

Naval Postgraduate School
Department of Oceanography
Monterey CA 93943-5000
Attn: Code 68, Dr. C. A. Collins

Naval Research Laboratory
Washington DC 20375
Attn: Commanding Officer

Naval Sea Systems Command HQ
Washington DC 20362-5101
Attn: Commander

Naval Postgraduate School
Monterey CA 93943
Attn: Superintendent
Dr. R. Renard, Chairman

Naval Surface Weapons Center
Dahlgren VA 22448-5000
Attn: Commander

Naval Surface Warfare Center/
White Oak
10901 New Hampshire Ave.
Silver Spring MD 20904-5000
Attn: Commander
Library

Naval Underwater Systems Center
Newport RI 02841-5047
Attn: Commander

Naval Underwater Systems Center
New London Laboratory
New London CT 06320
Attn: Officer in Charge

Naval Western Oceanography Center
Box 113
Pearl Harbor HI 96860-5050
Attn: CDR P. Kelley

NESDIS SRL
Washington DC 20233
Attn: (ERA1), Mr. P. McClain
(E/SP13), Mr. B. Pichel

NOAA-AOML
4301 Rickenbacker Causeway
Virginia Key FL 33149
Attn: Dr. G. Maul
Dr. P. Black

NOAA Data Buoy Center
Stennis Space Center MS 39529
Attn: Dr. G. Hamilton

NOAA Pacific Marine Env. Res. Lab.
7600 Sand Point Way NE
Seattle WA 98115-0070
Attn: Dr. M. McPhaden

Office of Naval Research
800 N. Quincy St.
Arlington VA 22217-5000
Attn: Code 10
Code 10D/10P, Dr. E. Silva
Code 112, Dr. E. Hartwig
Code 12
Code 120M, Mr. R. Peloquin

Office of Naval Research
ONR Branch Office
Box 39
FPO New York NY 09510-0700
Attn: Commanding Officer

Office of Naval Technology
800 N. Quincy St.
Arlington VA 22217-5000
Attn: Code 234, Dr. C. Votaw
Code 228, Dr. M. Briscoe

SAIC
Mail Stop 34, 10260 Campus Pt. Dr.
San Diego CA 92121
Attn: Dr. G. Innis
Ms. M. L. Morris

SAIC
205 Montecito Ave.
Monterey CA 93940
Attn: Mr. B. Mendenhall

SAIC
4900 Water's Edge Dr., Suite 510
Raleigh NC 27606
Attn: Dr. V. Waddel

Scripps Institution of Oceanography
La Jolla CA 92093
Attn: Dr. S. Pazan
Dr. W. White

Scripps Institution of Oceanography
University of California
P.O. Box 6049
San Diego CA 92106

Space and Naval Warfare
Systems Command
2511 Jeff Davis Hwy.
Washington DC 20363-5100
Attn: Commander
Code PMW 141, LCDR B. Cook
Code PMW 141,
CDR G. Trumbower

ST Systems Corporation
1577 Spring Hill Road, Suite 500
Vienna VA 22180
Attn: Mr. P. Gatje

University of Colorado
Dept. of Aerospace Eng. Sci.
Campus Box 429
Boulder CO 80309-0429
Attn: Dr. G. Born
Dr. W. Emery

University of Miami
Center for Marine Studies
4600 Rickenbacker Causeway
Miami FL 33149-1098
Attn: Dr. O. Brown

University of Oklahoma
Department of Meteorology
200 Felgar St.
Norman OK 73019
Attn: Dr. C. Duchon, Chairman

U.S. Naval Academy
Department of Oceanography
Annapolis MD 21402-5026
Attn: Chairman
Dr. A. Strong

U.S. Naval Observatory
34th St. & Massachusetts Ave., NW
Bldg. 1
Washington DC 20392-1800
Attn: Mr. D. Montgomery

University of Rhode Island
Graduate School of Oceanography
Narragansett Bay Campus
Narragansett RI 02882-1197
Attn: Dr. P. Cornillon

Woods Hole Oceanographic Institution
P.O. Box 32
Woods Hole MA 02543
Attn: Dr. C. Dorman, Director
Dr. J. Price

Joint Oceanographic Institute
1755 Mass. Ave., NW
Suite 800
Washington DC 20036
Attn: R. Tipper

NASA-JPL
MS 183-501
4800 Oak Grove Dr.
Pasadena CA 91109
Attn: Dr. D. Hagen

Coastal Studies Institute
Louisiana State University
Baton Rouge LA 70803-7527
Attn: Dr. O. Huh

Nansen Ocean & Remote
Sensing Center
Edv. Griegsr. 3A
N-5037 Solheimsvik
Norway
Attn: Dr. O. Johannessen

University of Washington
Atmospheric Sciences AK-40
Seattle WA 98195
Attn: Dr. K. Katsaros

REPORT DOCUMENTATION PAGE

Form Approved
OMB No. 0704-0188

1. Agency Use Only *(Leave blank).*	2. Report Date. May 1990	3. Report Type and Dates Covered. Final

4. Title and Subtitle.

Diurnal Ocean Surface Layer Model Validation

5. Funding Numbers.

Program Element No 63704N

Project No.

Task No

Accession No DN394457

6. Author(s).

Jeffrey D. Hawkins, D. May and Fred Abell*

7. Performing Organization Name(s) and Address(es).

Ocean Science Directorate
Naval Oceanographic and Atmospheric Research Laboratory
Stennis Space Center, Mississippi 39529-5004

8. Performing Organization Report Number.

NOARL Report 3

9. Sponsoring/Monitoring Agency Name(s) and Address(es).

Space and Naval Warfare Systems Command
Washington, DC

10. Sponsoring/Monitoring Agency Report Number.

11. Supplementary Notes.

*Sverdrup Technology, Inc.

12a. Distribution/Availability Statement.

Approved for public release; distribution is unlimited. Naval Oceanographic and Atmospheric Research Laboratory, Stennis Space Center, Mississippi 39529-5004.

12b. Distribution Code.

13. Abstract *(Maximum 200 words).*

The Diurnal Ocean Surface Layer (DOSL) model at the Fleet Numerical Oceanography Center forecasts the 24-hour change in global sea surface temperatures (SST). Validating the DOSL model is a difficult task due to the huge areas involved and the lack of in situ measurements. Therefore, this report details the use of satellite infrared multichannel SST imagery to provide day and night SSTs that can be directly compared to DOSL products. This water-vapor-corrected imagery has the advantages of high thermal sensitivity (0.12°C), large synoptic coverage (nearly 3000 km across), and high spatial resolution that enables diurnal heating events to be readily located and mapped.

Several case studies in the subtropical North Atlantic readily show that DOSL results during extreme heating periods agree very well with satellite-imagery-derived values in terms of the pattern of diurnal warming. The low wind and cloud-free conditions necessary for these events to occur lend themselves well to observation via infrared imagery. Thus, the normally cloud-limited aspects of satellite imagery do not come into play for these particular environmental conditions.

The fact that the DOSL model does well in extreme events is beneficial from the standpoint that these cases can be associated with the destruction of the surface acoustic duct. This so-called "afternoon effect" happens as the afternoon warming of the mixed layer disrupts the sound channel and the propagation of acoustic energy. Thus, the DOSL model can be used to help estimate the location of where the afternoon effect may occur, as well as help analysts interpret artificially induced, diurnal heating SST gradients when generating mesoscale front and eddy maps.

14. Subject Terms.

satellite SST, remote sensing, thermodynamic ocean models

15. Number of Pages. 18

16. Price Code.

17. Security Classification of Report.	18. Security Classification of This Page.	19. Security Classification of Abstract.	20. Limitation of Abstract.
Unclassified	Unclassified	Unclassified	None